



Photocatalytic hydroxylation of phenol to dihydroxybenzenes by TiO₂/RGO composites

Xili Shang^{1*}, Changhai Li¹, Meiling Liu², Ping Du^{1,3} and Jingjing Zheng¹

¹Department of Chemical Engineering, Binzhou University, Binzhou, China

²School of Chemical Engineering, Changchun University of Technology, Changchun, China

³Engineering Research Center for Industrial Waste Water Reclamation of Shandong Province, Binzhou University, Binzhou, China

ABSTRACT

Photocatalytic hydroxylation of phenol to dihydroxybenzenes (catechol and hydroquinone) in liquid phase over a novel heterogeneous photocatalyst TiO₂/Reduced Graphene Oxide was investigated with the assistance of light irradiation at room temperature. The catalysts were characterized by FT-IR, UV-vis DRS, SEM and XRD. The conversion of phenol could reach high up to 64.9%, with a total selectivity of 95% and the yield of 39.3%, 22.3% for catechol and hydroquinone, respectively.

Keywords: Dihydroxybenzenes, Photocatalytic, hydroxylation, Reduced Graphene Oxide

INTRODUCTION

Dihydroxybenzenes (DHB) are important intermediates used in spices, dyes, medicines and pesticides [1]. The hydroxylation of phenol with H₂O₂ to produce DHB (catechol and hydroquinone) has attracted much attention, and many homogeneous and heterogeneous catalysts have been studied [2]. Compared to the homogeneously catalyzed reaction, the heterogeneously catalyzed hydroxylation with solid catalysts has attracted more interest due to favorable properties of the catalysts (eco-friendly nature and catalyst recoverability) [3,4].

Hydroxylation of phenol with H₂O₂ over TS-1, which was first commercialized by Enichem in 1986 [5], was an alternative environmental friendly route, using methanol and acetone as the solvents at 353 K. The conversion of phenol could reach 25% in the Enichem route, which was much higher than the conversions reached in the Rhone-Poulenc route (5%) and Brichima route (10%). However, many problems still exist, such as the short lifetime and low output of the catalyst. Organic photocatalytic oxidations have been largely studied [6], despite the selectivity of these processes still remaining low [7]. Benzene, for instance, can undergo electrophilic attack by hydroxyl radicals and give rise to phenol as the primary product [8–10], the high reactivity of hydroxyl radicals making this process thermodynamically possible. Yamaguchi et al. [11] reported the liquid-phase oxidation of benzene in aqueous acetic acid solvent over V-substituted heteropolyacids (V-HPAs) using molecular O₂ and ascorbic acid. Phenol was exclusively obtained as the oxygenation product but the reuse of the V-HPA catalyst caused gradual deactivation for phenol formation. The use of vanadium grafted zeolites type Beta and ZSM-5 for direct oxidation of benzene to phenol was proposed by Dimitrova and Spassova [12]. Here, we present our preliminary data on Photocatalytic hydroxylation of phenol to dihydroxybenzenes by TiO₂/RGO Composites.

EXPERIMENTAL SECTION

2.1. Materials

Tetrabutyl titanate (TBT) was obtained from Jiangsu Yongli Chemical Co., Ltd. PR China. Dicyandiamide was

obtained from Aladdin Chemical Reagent Corp., PR China. Tetrabutyl titanate (TBT), hydrofluoric acid (40 wt.%), acetate acid (>99.8%) and tert-butyl alcohol (TBA) were purchased from Beijing Chem. Works, PR China. All chemicals were used as received without further purification, and ultrapure water (>18 M_Ω cm) obtained from Millipore system was used throughout all the experiments.

2.2. preparation of graphite oxide

The graphite oxide (GO) were prepared by Hummers' method. 1 g NaNO₃ and 2 g graphite was added into 46 mL H₂SO₄ in a three-neck flask with stirring for 1 h. Then 6 g KMnO₄ was added slowly into the mixture solution and kept stirring for 1 h at 0 °C. Sequentially, 30 ml deionized water was added and stirred for 30 min at 35 °C, The obtained mixture was kept stirring for another 1 h at 98 °C which was followed by adding 90 mL deionized water (60 °C) and 30 ml H₂O₂ aqueous solution (30%) successively. When the obtained mixture was cooled down to room temperature, 60 ml HCl aqueous solution (30%) was added in with stirring for 30 min. The obtained precipitate was purified by repeating dispersing in plenty of water by ultrasonic concussion and then centrifuging and finally drying.

2.3. preparation of TiO₂/RGO

The TiO₂/RGO composites were prepared by a modified hydrothermal method. A certain amount of the as-prepared GO was dispersed in 40 mL ethanol for ultrasonic stripping 1 h. Then 20 mL hydrochloric acid and deionized water of 10 mL was added, and ultrasonic oscillation for 1 h, then add 0.36 g H₂SO₄ under constant stirring by a magnetic stirrer, finally add TBT 4.3 mL slowly, continue stirring for 3 h. Continually, the mixed solution was shifted into a hydrothermal reactor, reaction for 24 h under certain temperature. Subsequently, the reaction solution was washed to neutral with ethanol and deionized water respectively, After desiccation by vacuum oven at 70 °C for 12 h, the obtained powder was annealed at certain temperature under a constant N₂ flow for 2 h. The mass ratio of GO : TBT was x (x = 0, 0.01, 0.02, 0.03 and 0.04) and these samples were designated as RGO, TiO₂/RGO-1, TiO₂/RGO-2, 0.6TiO₂/RGO-3, TiO₂/RGO-4.

2.4. Characterizations of TiO₂/RGO

To determine the crystal phase composition of TiO₂/RGO X-ray diffraction measurements were carried out using a X'Pert Pro X-ray diffractometer (PAN Analytical Co., Holland) with Cu K α radiation, the diffractograms were recorded in the 2 θ range 10°-80° with steps of 0.017°. The surface physical morphology of the TiO₂/RGO was observed by the transmission electron microscope (Tecnai G² F20, America). FT-IR spectra of pure TiO₂, RGO and the TiO₂/RGO were recorded on a Nicolet 380 FT - IR Spectrometer (Thermo Electron Co., America) and a KBr beam splitter within wavelength range of 400 - 4000 cm⁻¹. UV - Vis diffuse reflectance spectra of TiO₂ and TiO₂/RGO were performed using a Perkin Elmer Lambda 750 spectrophotometer (Perkin Elmer Co., America).

2.5. Hydroxylation of phenol

Hydroxylation of phenol was carried out in XPA-7 photochemical reactor (Jiangsu, China). A certain amount of catalyst, phenol, deionized water, acetonitrile (cosolvent) and H₂O₂ was added into the reactor gradually with stirring under 20 °C, and continue stirring for 20 min to keep adsorption equilibrium, and then turn on the light, which in parallel to the reactor. The samples were collected at regular intervals of time, centrifuged and analyzed by Waters 2995 liquid chromatography. The conversion of phenol (C_{PH}), yield of catechol (Y_{CAT}), yield of hydroquinone (Y_{HQ}), and selectivity of dihydroxybenzenes (S_{DHB}) were calculated as follows:

$$C_{PH} = \frac{\text{mole of phenol reacted}}{\text{initial mole of phenol}} \times 100\%$$

$$Y_{CAT} = \frac{\text{mole of catechol produced}}{\text{initial mole of phenol}} \times 100\%$$

$$Y_{HQ} = \frac{\text{mole of hydroquinone produced}}{\text{initial mole of phenol}} \times 100\%$$

$$S_{DHB} = \frac{\text{yield of catechol} + \text{yield of hydroquinone}}{\text{conversion of phenol}} \times 100\%$$

RESULTS AND DISCUSSION

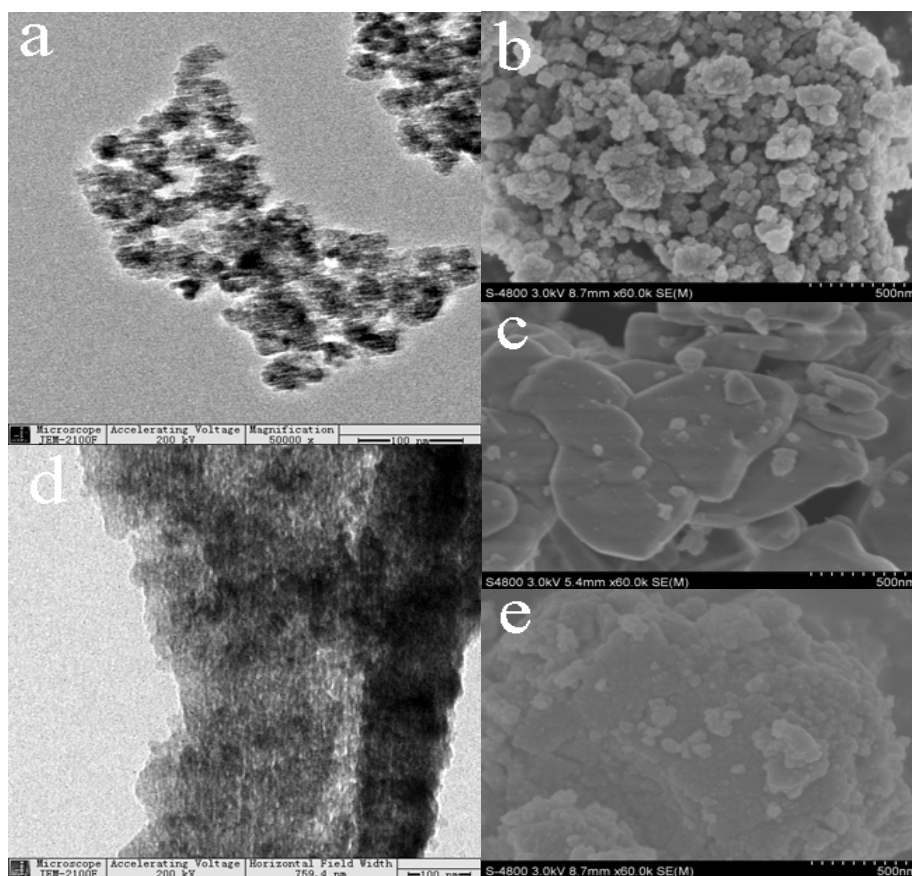
3.1 Morphology of TiO₂/RGO

Fig. 1. TEM image (a) and SEM image (b) of pure TiO₂; SEM image of the GO (c); TEM image (d) and SEM image (e) of RGO/TiO₂

The morphology and structure of the pure TiO₂, GO and TiO₂/RGO are displayed in Fig. 1. Fig. 1a, b show that the pure TiO₂ has a favorable dispersibility. Fig. 1c shows the obvious layer structure of GO. And Fig. 1 d shows that the TiO₂ nanoparticles are well dispersed and uniformly anchored on the RGO sheet. The SEM image (Fig. 1d) of the TiO₂/RGO sample demonstrates the homogeneity of the composite in a large scale. In particular, only a small portion of RGO sheets and trace amount of freestanding TiO₂ can be observed, while most of the surfaces of the RGO sheets are covered by the TiO₂ nanoparticles. Also, most of the TiO₂ particles are anchored on the surfaces of RGO sheets, which is beneficial to efficient electron collection during the photocatalytic reaction processes.

3.2 UV-Vis DRS study

Fig. 2 shows the UV-Vis diffuse reflectance spectra (UV-Vis DRS) of pure TiO₂, GO and TiO₂/RGO. Obviously, there was no absorption above 400 nm for pure TiO₂, while TiO₂/RGO shows clear visible light absorption from 400 to 600 nm, and GO has strong absorption in both visible and ultraviolet region. While the absorption capability of TiO₂/RGO was weak than that of pure TiO₂ in the UV region of 200-350 nm, but strong in visible light region of 400-700 nm, which may be due to the synergistic effect caused by graphite alkene and TiO₂ [13], all of which prove that the TiO₂/RGO may has good visible light photocatalytic performance.

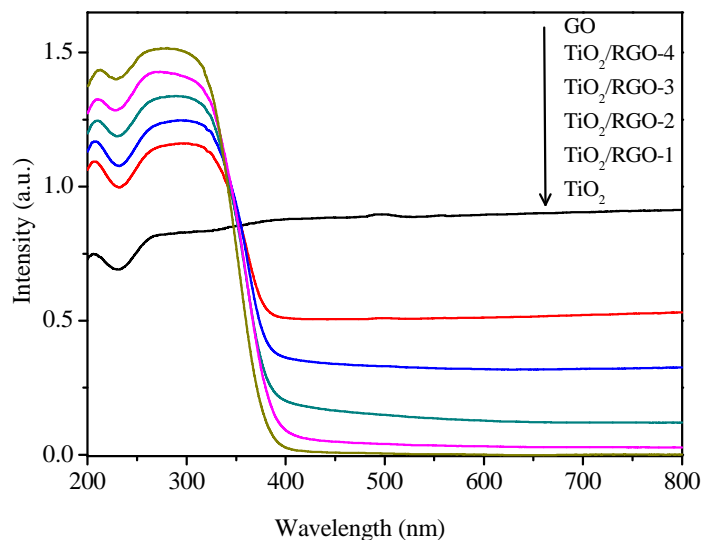


Fig. 2. The UV-Vis diffuse reflectance spectra of pure TiO₂, GO and TiO₂/RGO

3.3 FT-IR study

The functionalization of TiO₂ on the surface of RGO sheets and the reduction process of GO were also confirmed by FT-IR. The FT-IR spectrum of GO, TiO₂ and TiO₂/RGO are shown in Fig. 3. The peaks of 3400 cm⁻¹ (OH), 1739 cm⁻¹ (C = O), 1227 cm⁻¹ (C-O-C) and 1056 cm⁻¹ (C-O) are appeared prove that the graphite was oxidized to GO. Existence of these oxygen-containing functional groups making the GO has good hydrophilicity, and meanwhile the layer distance of GO was increased obviously compared with flake graphite. after calcined the peak at 1227 cm⁻¹ of the GO was disappeared, and the peak at 1030 cm⁻¹ decreased significantly, all of which show that most of the surface oxygen-containing functional groups disappeared, GO was reduced to RGO. From Fig. 3 characteristics of TiO₂/RGO has obvious absorption peak of TiO₂, and no obvious peaks of oxygen-containing functional groups, indicating that GO has been reduced to RGO.

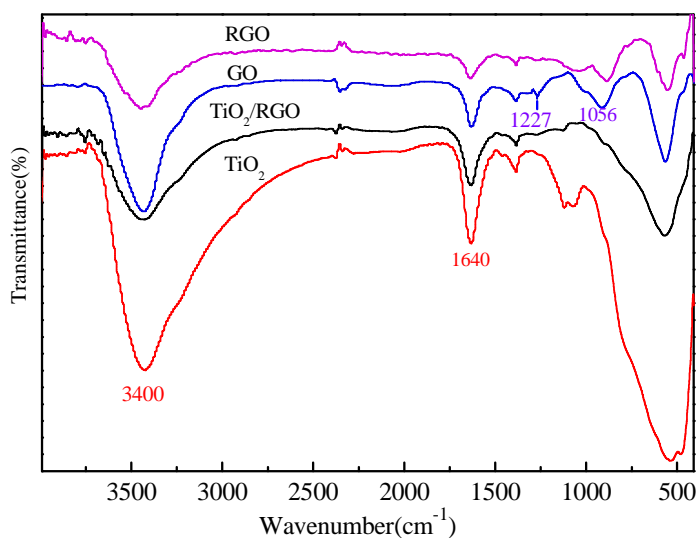


Fig. 3. FT-IR spectra of samples

3.4 XRD study

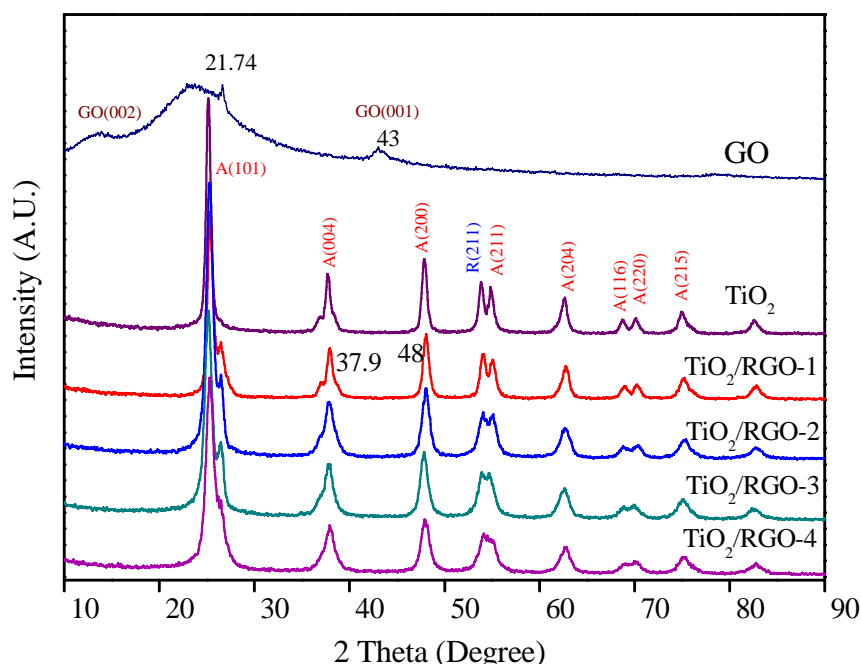


Fig. 4. XRD patterns of GO, pure TiO₂ and TiO₂/RGO

Fig. 4 shows XRD patterns of GO, pure TiO₂ and TiO₂/RGO composites with different mass ratios of RGO. All the samples of TiO₂/RGO-x exhibit similar XRD patterns with pure TiO₂. Diffraction angles of TiO₂ in XRD correspond to the crystal planes of anatase TiO₂ and rutile TiO₂. From Fig. 4 we can also see the XRD pattern of GO with a characteristic (002) peak at $2\theta = 13.86^\circ$, and a characteristic (001) peak at $2\theta = 43.04^\circ$. Compared to GO, complete disappearance of the strong (002) peak in TiO₂/RGO composites suggests successful conversion of GO to RGO in the final composites. Notably, no typical diffraction peaks belonging to the separate graphene are observed in the TiO₂/RGO composites. The reason can be ascribed to the much lower crystalline extent of graphene than that of TiO₂, which results in the shielding of the graphene peaks by those of TiO₂ [14, 15]. Furthermore, the crystallization peaks of the materials have not changed its position but broaden, illustrate that the join of the RGO has no effect on the crystalline types of TiO₂. The calculated average TiO₂ crystallite sizes of these particles using Scherrer's formula are 12.8, 11.2, 8.5, 7.8 and 7.6 nm, corresponding to TiO₂, TiO₂/RGO-1, TiO₂/RGO-2, TiO₂/RGO-3 and TiO₂/RGO-4, respectively, which indicates that the particle size of the samples decreases with the RGO addition increased. As we all know, the smaller the sizes of catalyst particles, the larger the size of the specific surface area, faster the photoinduced electronic can get to the surface of the catalyst, this is one reason that TiO₂/RGO show higher photocatalytic activity compared with pure TiO₂.

3.5 Photocatalytic hydroxylation activity

The photocatalytic activity of GO, pure TiO₂ and TiO₂/RGO composites were measured by photocatalytic hydroxylation of phenol in aqueous solution under light irradiation. the products were analyze by LC as shown in Fig. 5.

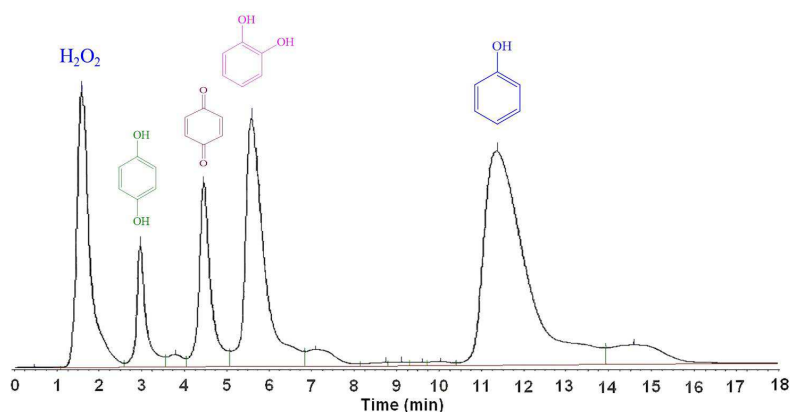


Fig. 5. Liquid chromatography spectra of phenol photocatalysis on three catalysts under UV radiation. phenol 1.5g, H₂O 45.0 mL

The control experiment confirms that in the absence of UV irradiation, phenol was not converted to catechol and hydroquinone even with adding excessive H₂O₂. It is clear from Fig. 5 that Another point to note is that controlling the capacity of RGO significantly enhanced the selectivity toward objective DHB (catechol and hydroquinone). Phenol conversion could reach high up to 64.9%, with a total selectivity of 95% and the yield of 39.3%, 22.3% for catechol and hydroquinone, respectively in the existence of TiO₂/RGO-3. It indicated that the interactions between RGO sheets and TiO₂ can greatly promote the photocatalytic activity.

Table 1 The photocatalytic activity of different photocatalysts

Catalyst type	X _(pH) (%)	Y(HQE)(%)	Y(CAL) (%)	S(%)
TiO ₂	66.9	4.6	12.6	25.7
TiO ₂ /RGO-1	92.1	11.2	19.8	33.6
TiO ₂ /RGO-2	92.7	29.8	20.1	53.8
TiO ₂ /RGO-3	93.2	41.7	23.6	70.1
TiO ₂ /RGO-4	93.1	35.5	21.4	61.1

Phenol, 1.5 g; H₂O, 15.0 mL; H₂O₂, 3.0 mL. Irradiation time, 4.0 h.

CONCLUSION

In summary, TiO₂/RGO composites with improved photocatalytic activity for hydroxylation of phenol were successfully synthesized by a modified hydrothermal method. XRD showed that TiO₂/RGO exhibit similar XRD patterns with anatase TiO₂ and rutile TiO₂. The photocatalytic hydroxylation experiments demonstrated that most of the TiO₂/RGO composites exhibit much better photocatalytic performance than pure TiO₂. The TiO₂/RGO-3 sample possesses the highest hydroxylation efficiency, phenol conversion could reach high up to 64.9%, with a total selectivity of 95% and the yield of 39.3%, 22.3% for catechol and hydroquinone, respectively. The well established interfacial interaction and largely enhanced charge transfer efficiency should be responsible for the improved photocatalytic activity.

Acknowledgments

This work was supported by the Project of Shandong Province Higher Educational Science and Technology Program (J12L64). Binzhou city Science & Technology Development Program (2013ZC1602) and Binzhou university scientific research projects (2013ZDL03, BZXYZZJJ201403 and BZXYFB20120603).

REFERENCES

- [1] K Weissermel; HJ Arpe. *Industrial Organic Chemistry*, VCH, Weinheim, **1993**; 391-395.
- [2] S Li; GL Li; GY Li, et al. *Micropor Mesopor Mat.*, **2011**, 143: 22-29.
- [3] LL Lou; SX Liu, *Catal. Commun.*, **2005**, 6: 762.
- [4] S Kulawong; S Prayoonpokarach; A. Neramittagapong, et al. *J. Ind. Eng. Chem.*, **2011**, 17: 346.
- [5] U Romano; A Esposito; F. Maspero, et al. *Stud. Surf. Sci. Catal.* **55** (1990) 33-41.
- [6] A Maldotti; ARA Molinari. *Chem. Rev.* **2012**, 102: 3811-3836.
- [7] A Maldotti; A Molinari; R Amadelli, et al. *Photochem. Photobiol.Sci.* **2008**, 7: 819-825.
- [8] DH Bremner; AE Burgess; FB Li. *Appl. Catal. A: Gen.* **2000**, 203: 111-120.
- [9] K Otsuka; M Kunieda; H Yamagata. *J. Electrochem. Soc.* **1992**, 139: 2381-2386.
- [10] G Palmisano; M Addamo; V Augugliaro, et al. *Catal. Today*, **2007**, 122: 18-127.
- [11] S Yamaguchi; S Sumimoto; Y Ichihashi, et al. *Ind. Eng. Chem. Res.* **2005**, 44: 1-7.
- [12] R Dimitrova; M Spassova. *Catal. Commun.* **2007**, 8: 693-696.
- [13] K Kamiya; S Sakka; K Terada. *Mater. Res. Bull.*, **1977**, 12(11): 1095-1102.
- [14] YH Zhang; ZR Tang; XZ Fu, et al. *ACS Nano*, **2010**, 4: 7303-7314.
- [15] P Wang; J Wang; XF Wang, et al. *Appl. Catal. B*, **2013**, 132-133: 452-459.